ENGINEERING TRANSACTIONS • *Engng. Trans.* • **57**, 1, 3–15, 2009
Polish Academy of Sciences • Institute of Fundamental Technological Research

DYNAMIC BUCKLING OF NON-SWAY IMPERFECT RECTANGULAR STEEL FRAMES

I. G. Raftoyiannis [1)], A. N. Kounadis [2)]

[1)] **National Technical University of Athens**
Department of Civil Engineering
9 Iroon Polytechneiou St., Zografou Campus
Athens 15780, Greece

[2)] **Academy of Athens**
Biomedical Research Foundation
4 Soranou Efessiou, Athens 11527, Greece

A nonlinear stability analysis is performed on non-sway rectangular two-bar steel frames subjected to a concentrated, suddenly applied joint load with constant magnitude and infinite duration. Using energy and geometric considerations, the dynamic buckling load is determined by considering the frame, being a continuous system, as a discrete 2 degrees-of-freedom system with corresponding coordinates of the two bar axial forces. The effect of imperfection sensitivity due to loading eccentricity is also addressed. A qualitative and quantitative analysis of these autonomous systems yields a substantial reduction of the computational work. The efficiency and reliability of the nonlinear stability analysis proposed herein is illustrated by several examples, which are also solved using finite element nonlinear analysis.

Key words: nonlinear dynamic stability, imperfect frames, suddenly applied load, loading eccentricity, FEM.

1. Introduction

In modern elastomechanics, *elastic stability theory* has attracted considerable attention due to the increasing demands in the design and analysis of light and stiff structures with high load-carrying capacity. A major contribution to this area is the initial post-buckling analysis of Koiter [1], which refers to systems that in their ideally perfect state exhibit a bifurcation point at the critical buckling load. However, the existence of ideally perfect structural systems is an exception rather than the rule. The majority of real structural systems, if accurately modeled, experiences limit point instability rather than bifurcational buckling. This is so because the presence of any small imperfection, which is unavoidable in actual systems, implies the degeneration of the bifurcation to a limit point [2].

The present work examines in detail the critical dynamic buckling response of non-sway, imperfect (due to loading eccentricity) two-bar frames, which are supported on two immovable hinges. It is qualitatively shown that this type of non-sway frames, associated from the onset of loading with (primary) bending, cannot exhibit any asymmetric bifurcation, losing always its stability via a limit point. However, the case of loss of stability via any asymmetric bifurcation can be considered only in an asymptotic sense. The first buckling load estimate, useful for the subsequent development, is readily obtained by employing a linear stability analysis. Thereafter, the nonlinear equilibrium equations of the latter frame are derived through a variational approach by employing the principle of stationary value of the total potential energy (TPE). These equations can be written in terms of the first derivatives of the TPE with respect to the unknown axial forces in the two bars. This is an important step, which facilitates the analysis, since we can consider the continuous system (i.e. the two-bar frame) as a two-degrees-of-freedom model, governed by two generalized coordinates, being the aforementioned axial forces in the two bars. Then, one can establish the second variation of the TPE as a function of the above mentioned two axial forces. By vanishing the stability determinant (i.e. the second variation of the TPE), written in terms of the second derivatives of the TPE, we obtain the condition governing the critical state [7, 12]. This condition, along with the equilibrium equations, leads to an easy and direct evaluation of the critical (buckling) load. Moreover, simultaneous vanishing of the TPE and the equilibrium equations lead to a lower bound estimate of the dynamic buckling load. This very simple procedure yields reliable results for structural design, proposed for the above type of dynamic loading associated with autonomous systems. Subsequently, more reliable results for the dynamic buckling load are obtained using the energy and geometric considerations of KOUNADIS approach recently presented in Ref. [16].

The methodology proposed herein is demonstrated by means of several numerical examples solved also by a nonlinear FEM, which subsequently are compared with those of previous analyses [8, 9].

2. Mathematical formulation

Consider the rectangular two-bar, geometrically perfect, frame ABC shown in Fig. 1 supported on two immovable hinges. Let ℓ_i, A_i and I_i be the length, cross-sectional area, and moment of inertia of the i-th bar ($i = 1, 2$). The frame is loaded at its joint B by a vertical concentrated force P, eccentrically applied with respect to the centerline of the vertical bar AB. The loading eccentricity e^* measured from the axis of the latter bar is positive if the point of application of the load is located to the right of this axis. The deformed configuration of the frame is described by the displacements w_i^* (transverse deflection) and ξ_i^* (axial

displacement) at any point x_i^* of the centerline of the i-th bar. Both bars made of a Hookean material can undergo moderate rotations but small strains [4, 10, 11].

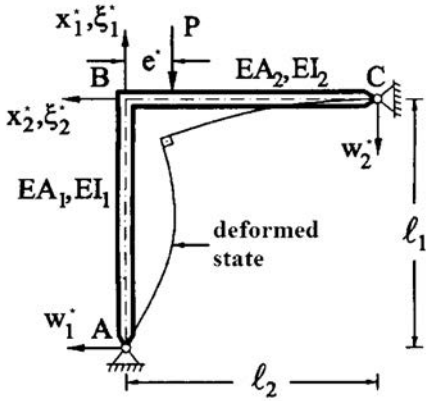

FIG. 1. Geometry and sign convention of an imperfect rectangular two-bar frame.

Introducing the dimensionless quantities

$$x_i = \frac{x_i^*}{\ell_i}, \quad w_i = \frac{w_i^*}{\ell_i}, \quad \xi_i = \frac{\xi_i^*}{\ell_i}, \quad k_i^2 = \frac{S_i \ell_i^2}{EI_i}, \quad \lambda_i^2 = \frac{A_i \ell_i^2}{I_i} \ (i = 1, 2),$$
$$e = \frac{e^*}{\ell_1}, \quad \beta^2 = \frac{P\ell_1^2}{EI_1}, \quad \rho = \frac{\ell_2}{\ell_1}, \quad \mu = \frac{I_2}{I_1}, \tag{2.1}$$

the total potential energy (TPE) function V, in dimensionless form, is given by KOUNADIS [5]:

$$V = \frac{1}{2}\int_0^1 \left[\lambda_1^2\left(\xi_1' + \frac{1}{2}w_1'^2\right)^2 + w_1''^2\right] dx_1 + \frac{\mu}{2\rho}\int_0^1 \left[\lambda_2^2\left(\xi_2' + \frac{1}{2}w_2'^2\right)^2 + w_2''^2\right] dx_2 + \beta^2\xi_1(1) + \beta^2\rho e w_2'(1), \tag{2.2}$$

where the prime denotes differentiation with respect to x_i $(i = 1, 2)$. Note that the replacement of the eccentric joint load by a centrally applied load and a bending moment – related to the last term of Eq. (2.2) – presupposes that e is sufficiently small.

The geometric boundary conditions, known a priori, are given by

$$w_1(0) = w_2(0) = \xi_1(0) = \xi_2(0) = 0,$$
$$w'_1(1) = w_2'(1), \qquad \rho\xi_2(1) = w_1(1), \qquad \xi_1(1) = -\rho w_2(1). \tag{2.3}$$

Application of the principle of a stationary value of the TPE function, $\delta V = 0$, yields the following differential equations:

$$\left.\begin{aligned} \lambda_i^2 \left(\xi_i' + \frac{1}{2} w_i'^2\right)' &= 0 \\ w_i'''' - \left[\left(\xi_i' + \frac{1}{2} w_i'^2\right) w_i'\right]' &= 0 \end{aligned}\right\} i = 1, 2 \tag{2.4}$$

and natural boundary conditions after using Eqs. (2.3)

$$\begin{aligned} w_1''(0) = w_2''(0) = 0, \\ \lambda_1^2 \left[\xi_1'(1) + \frac{1}{2} w_1'^2(1)\right] + \frac{\mu}{\rho^2} \left\{ w_2'''(1) - \lambda_2^2 \left[\xi_2'(1) \right.\right. \\ \left.\left. + \frac{1}{2} w_2'^2(1)\right] w_2'(1) \right\} + \beta^2 = 0, \\ \frac{\mu}{\rho^2} \lambda_2^2 \left[\xi_2'(1) + \frac{1}{2} w_2'^2(1)\right] - w_1'''(1) + \lambda_1^2 \left[\xi_1'(1) \right. \\ \left. + \frac{1}{2} w_1'^2(1)\right] w_1'(1) = 0, \\ w_1''(1) + \frac{\mu}{\rho} w_2''(1) + \rho \beta^2 e = 0. \end{aligned} \tag{2.5}$$

Integration of the first of Eqs. (2.4) gives

$$\xi_i'(x_i) + \frac{1}{2} w_1'^2(x_i) = -\frac{k_i^2}{\lambda_i^2} \qquad (i = 1, 2), \tag{2.6}$$

due to which the second of Eqs. (2.4) becomes

$$w_i''''(x_i) + k_i^2 w_i''(x_i) = 0 \qquad (i = 1, 2). \tag{2.7}$$

The general integrals of Eqs. (2.6) and (2.7) are

$$\begin{aligned} \xi_1(x_1) &= C - \frac{k_1^2}{\lambda_1^2} x_1 - \frac{1}{2} \int_0^{x_1} w_1'^2(x_1') dx_1', \\ \xi_2(x_2) &= \overline{C} - \frac{k_2^2}{\lambda_2^2} x_2 - \frac{1}{2} \int_0^{x_2} w_2'^2(x_2') dx_2', \\ w_1(x_1) &= C_1 \sin k_1 x_1 + C_2 \cos k_1 x_1 + C_3 x_1 + C_4, \\ w_2(x_2) &= \overline{C}_1 \sin k_2 x_2 + \overline{C}_2 \cos k_2 x_2 + \overline{C}_3 x_2 + \overline{C}_4, \end{aligned} \tag{2.8}$$

where the integration constants C, $\overline{C}$, C_i and $\overline{C}_i$ (for $i = 1, .., 4$) are determined by the boundary conditions.

Note that the unusual case of tension in the horizontal bar is not important. As shown by KOUNADIS *et al.* [8], this occurs for very small values of the external loading or in case of monotonically rising (stable) equilibrium paths.

Using Eqs. (2.6), the conditions (2.5), after taking into account that

$$w_1'''(x_1) + k_1^2 w_1'(x_1) = C_3 k_1^2$$

and

$$w_2'''(x_2) + k_2^2 w_2'(x_2) = \overline{C}_3 k_2^2,$$

are simplified as follows:

$$\begin{aligned} w_1''(0) = w_2''(0) &= 0, \\ k_2^2 \overline{C}_3 + \frac{\rho^2}{\mu}(\beta^2 - k_1^2) &= 0, \\ k_1^2 C_3 + \frac{\mu}{\rho^2} k_2^2 &= 0, \\ w_1''(1) + \frac{\mu}{\rho} w_2''(1) + \rho\beta^2 e &= 0. \end{aligned} \tag{2.9}$$

By virtue of the first four of geometric conditions (2.3) and the first two of conditions (2.8), we find $C = \overline{C} = C_2 = \overline{C}_2 = C_4 = \overline{C}_4 = 0$. Then, Eqs. (2.8) become

$$\begin{aligned} \xi_1(x_1) &= -\frac{k_1^2}{\lambda_1^2} x_1 - \frac{1}{2} \int_0^{x_1} w_1'^2(x_1') dx_1', \\ \xi_2(x_2) &= -\frac{k_2^2}{\lambda_2^2} x_2 - \frac{1}{2} \int_0^{x_2} w_2'^2(x_2') dx_2', \\ w_1(x_1) &= C_1 \sin k_1 x_1 + C_3 x_1, \\ w_2(x_2) &= \overline{C}_1 \sin k_2 x_2 + \overline{C}_3 x_2. \end{aligned} \tag{2.10}$$

Using the last two of Eqs. (2.10), the last one of the natural boundary conditions (2.9) and the fifth of geometric conditions (2.3), we obtain

$$\begin{aligned} C_1 k_1^2 \sin k_1 + \frac{\mu}{\rho} \overline{C}_1 k_2^2 \sin k_2 - \rho\beta^2 e &= 0, \\ C_1 k_1 \cos k_1 + C_3 - \overline{C}_1 k_2 \cos k_2 - \overline{C}_3 &= 0. \end{aligned} \tag{2.11}$$

The third and fourth of Eqs. (2.10) along with Eqs. (2.11) yield

$$C_1 = \frac{\rho\beta^2 e\cos k_2 + \dfrac{\mu}{\rho}\left[\dfrac{\rho^2}{\mu}\dfrac{\left(k_1^2-\beta^2\right)}{k_2^2} + \dfrac{\mu}{\rho^2}\dfrac{k_2^2}{k_1^2}\right]k_2\sin k_2}{k_1\left(k_1\sin k_1\cos k_2 + \dfrac{\mu}{\rho}k_2\cos k_1\sin k_2\right)},$$

(2.12)

$$\overline{C}_1 = \frac{\rho\beta^2 e\cos k_1 - \left[\dfrac{\rho^2}{\mu}\dfrac{\left(k_1^2-\beta^2\right)}{k_2^2} + \dfrac{\mu}{\rho^2}\dfrac{k_2^2}{k_1^2}\right]k_1\sin k_1}{k_2\left(k_1\sin k_1\cos k_2 + \dfrac{\mu}{\rho}k_2\cos k_1\sin k_2\right)},$$

$$C_3 = -\frac{\mu}{\rho^2}\frac{k_2^2}{k_1^2}, \overline{C}_3 = \frac{\rho^2}{\mu}\frac{\left(k_1^2-\beta^2\right)}{k_2^2}.$$

The last two of geometric conditions (2.3) yield the nonlinear equilibrium equations, which due to Eqs. (2.10), become

$$C_1\sin k_1 + C_3 = \rho\left[-\frac{k_2^2}{\lambda_2^2} - \frac{1}{2}\int_0^1 w_2'^2 dx_2\right],$$

(2.13)

$$\rho(\overline{C}_1\sin k_2 + \overline{C}_3) = \frac{k_1^2}{\lambda_1^2} + \frac{1}{2}\int_0^1 w_1'^2 dx_1,$$

where

$$\int_0^1 w_1'^2 dx_1 = C_3^2 + 2C_1C_3\sin k_1 + \frac{C_1^2k_1^2}{2}\left(1+\frac{\sin 2k_1}{2k_1}\right),$$

(2.14)

$$\int_0^1 w_2'^2 dx_2 = \overline{C}_3^2 + 2\overline{C}_1\overline{C}_3\sin k_2 + \frac{\overline{C}_1^2k_2^2}{2}\left(1+\frac{\sin 2k_2}{2k_2}\right),$$

with C_i and $\overline{C}_i$ $(i=1,3)$ given in Eqs. (2.12).

By virtue of relations (2.12) and (2.14), Eqs. (2.13) yield two nonlinear equilibrium equations with respect to k_1^2 and k_2^2, which can be determined only numerically as functions of the external loading β^2 for given values of the parameters $\lambda_i (i=1,2)$, ρ, μ and e. The entire (prebuckling and postbuckling) equilibrium path, being of the implicit form:

$$\beta^2 = \beta^2(k_1, k_2; \lambda_1, \lambda_2, \rho, \mu, e), \tag{2.15}$$

is established only numerically by solving Eqs. (2.13) with respect to k_i $(i = 1, 2)$ for various levels of the load β^2 and given values of λ_1, λ_2, μ, ρ and e, and then by plotting it via the relationship β^2 versus k_i $(i = 1, 2)$ or, usually, β^2 versus $w_1(1)$, $w_1'(1)$, $\xi_1(1)$ or $\xi_2(1)$.

3. Static critical loads

Introducing into Eq. (2.2) the expressions given in Eqs. (2.10), after integration, we get the expression of the TPE function V in terms of the unknown axial forces k_1 and k_2, for given values of the parameters λ_i $(i = 1, 2)$, μ, ρ and e. The derivatives of V with respect to k_1 and k_2, denoted by V_1 and V_2, yield the two nonlinear equilibrium Eqs. (2.13), i.e.

$$\begin{aligned} V_1 &= C_1 \sin k_1 + C_3 + \rho \left[\frac{k_2^2}{\lambda_2^2} + \frac{1}{2} \int_0^1 w_2'^2 dx_2 \right] = 0, \\ V_2 &= \rho(\overline{C}_1 \sin k_1 + \overline{C}_3) - \left[\frac{k_1^2}{\lambda_1^2} + \frac{1}{2} \int_0^1 w_1'^2 dx_1 \right] = 0, \end{aligned} \tag{3.1}$$

where C_1, C_3, $\overline{C}_1$ and $\overline{C}_3$ are given by Eqs. (2.12), and the integrals by relations (2.14).

The critical state C (β_c, k_1^c, k_2^c) is obtained by the condition of vanishing of the determinant of the matrix $[V_{ij}]$ of the second variation $\delta^2 V^c$, evaluated at the critical state C, namely

$$\det[V_{ij}]^c = \left(V_{11}V_{22} - V_{12}^2\right)^c = 0, \tag{3.2}$$

where

$$\begin{aligned} V_{11} &= \partial^2 V / \partial k_1^2, \\ V_{22} &= \partial^2 V / \partial k_2^2, \\ V_{12} &= V_{21} = \partial^2 V / \partial k_1 \partial k_2. \end{aligned}$$

4. Dynamic critical loads

Such an autonomous system, if damping is ignored, is governed by the principle of conservation of total potential energy, TPE, Hamiltonian E between any two states, i.e.

$$E = K + V, \tag{4.1}$$

where K is the positive definite total kinetic energy and V is the TPE, respectively. For this undamped autonomous system under the above type of dynamic loading, the initial ($t = 0$) conditions imply zero displacements and velocities, which yield $K_{t=0} = V_{t=0} = 0$ and hence $E = 0$. Since throughout the motion $E = 0$, from Eq. (4.1) it follows that [3, 6, 14]

$$V = -K. \tag{4.2}$$

Namely, throughout the motion (including the instant of Dynamic Buckling) the TPE function V is negative (i.e. for $V > 0$ there is no motion, and thus no dynamic buckling). According to the Lagrange or Laplace dynamic global stability criterion [16], *dynamic buckling* (in the large) for autonomous systems is defined as that state for which an escaped motion becomes either unbounded or of a very large amplitude. The minimum load corresponding to this state is defined as dynamic buckling load (DBL).

For 1-DOF autonomous undamped systems, dynamic buckling occurs always through a *saddle* (equilibrium) point, and hence $K = 0$, which due to Eq. (4.2) yields $V = 0$. The exact DBL and the associated critical displacement are obtained by solving the system of Eqs. $V = V_1 = 0$.

For 2-DOF systems the DBL is obtained by the procedure presented in Ref. [16, 17]. A lower bound dynamic buckling load denoted by $\tilde{\beta}_D^2$ is obtained by the solution of Eq. (3.1) and $V = 0$.

5. Numerical results

Numerical results for various geometric configurations of frames are given in both the graphical and tabular forms. Figures 2 and 3 show the total potential energy $V = 0$ in the $w_1(1)$–$w_2(1)$ plane for various load levels β^2, for a rectangular frame with

$$\mu = \rho = 1,$$

$$\lambda_1 = \lambda_2 = 80$$

and loading eccentricity $e = 0.01$. Note that $V = 0$ represents a closed curve in the $w_1(1)$–$w_2(1)$ plane for load levels lower than $\beta^2 = 2.2149$ (Fig. 3a). For higher loads, $V = 0$ represents an open curve (Fig. 2b) in the aforementioned plane. The motion of the joint B is bounded for load levels lower than $\beta^2 = 2.4585$, becoming unbounded for higher loads. The solution technique for obtaining the V-curve is based on the Newton-Ralphson scheme, where the symbolic manipulator Mathematica 5.1 [13] has been employed. The joint motion is obtained by means of a FEM nonlinear solution.

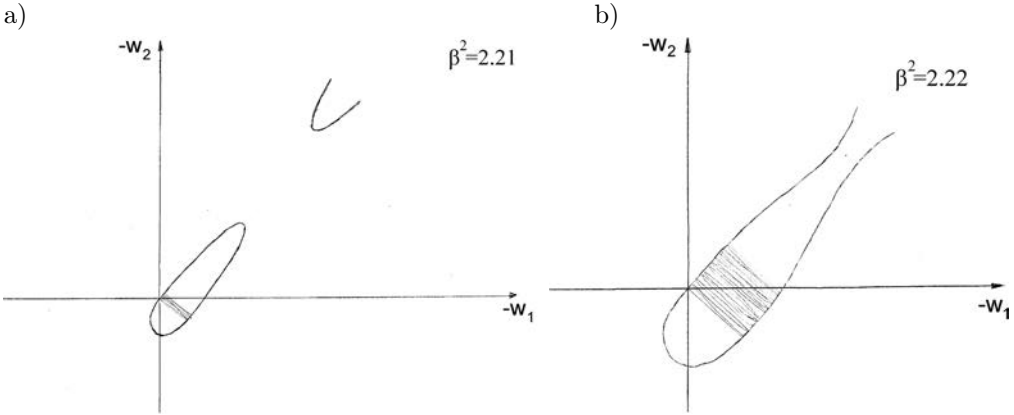

FIG. 2. Total potential energy V vs. $w_1(1)$–$w_2(1)$ for:
a) $\beta^2 = 2.21$ and b) $\beta^2 = 2.22$.

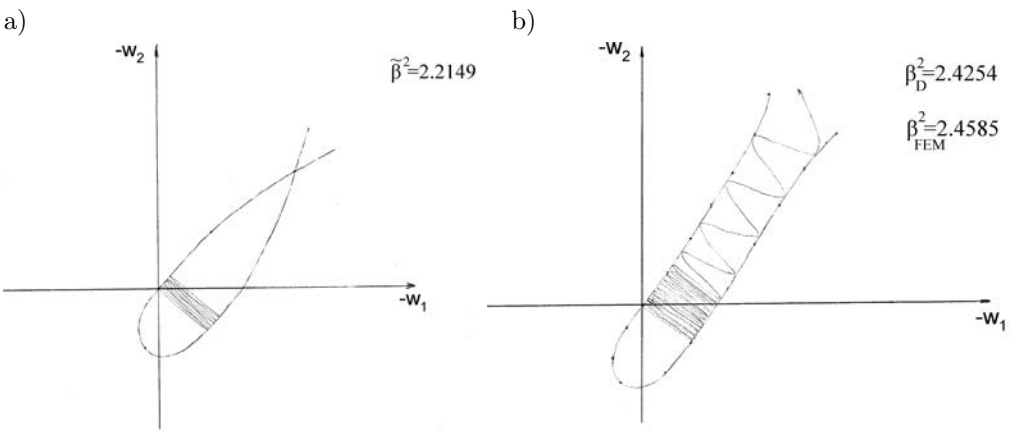

FIG. 3. Total potential energy V vs. $w_1(1)$–$w_2(1)$ for:
a) $\beta^2 = \tilde{\beta}^2 = 2.2149$ and b) $\beta_D^2 = 2.4254$.

In Table 1, one can see numerical values of the lower bound critical loads $\tilde{\beta}_D^2$ and the analytical and numerical dynamic buckling loads (DBL) β_D^2 with the corresponding values of loading eccentricities, slenderness ratios, moment of inertia and length ratios.

It is worth to mention that the maximum deviation in β^2 between the present analytical approach and the FEM results is less than 1.3%. However, the method proposed herein is less cumbersome and very efficient in parametric studies and can be more readily applied than a numerical FEM nonlinear analysis. The entire analysis is also facilitated by using qualitative considerations based on sufficient knowledge of the physical phenomenon of the problem under discussion.

Table 1. Critical DBL β^2 for loading eccentricity $e = 0.01$ and various values of μ, ρ, λ_1.

λ_1	μ	ρ	$\tilde{\beta}_D^2$	β_D^2
40	0.25	0.25	2.0189	2.2108 (2.2409)
		1	0.8909	0.9755 (0.9888)
		4	0.2626	0.2876 (0.2915)
	1	0.25	2.9596	3.2409 (3.2851)
		1	2.1745	2.3811 (2.4136)
		4	0.8949	0.9799 (0.9933)
	4	0.25	3.3251	3.6411 (3.6908)
		1	3.2985	3.6120(3.6613)
		4	2.1929	2.4013 (2.4340)
80	0.25	0.25	2.0564	2.2519 (2.2826)
		1	0.9074	0.9937 (1.0072)
		4	0.2675	0.2929 (0.2969)
	1	0.25	3.0146	3.3012 (3.3462)
		1	2.2149	2.4254 (2.4585)
		4	0.9115	0.9981 (1.0118)
	4	0.25	3.3869	3.7088 (3.7594)
		1	3.3598	3.6791 (3.7294)
		4	2.2336	2.4459 (2.4793)

Note: The values in parentheses correspond to results obtained by FEM.

A nonlinear finite element (FEM) analysis is also employed for obtaining the critical loads and studying the postbuckling behavior of the frame. For this purpose, the finite element package Algor is utilized [15]. With the aid of the "Superdraw" editor of Algor, the frame is modeled as a plane model in the XY-plane, where all out-of-plane displacements are restrained. Both the column and the beam are subdivided into 100 beam elements. Thus, the frame model has 602 degrees of freedom and 200 elements. Next, the boundary conditions (pinned supports) and the beam properties (material and sectional properties) are defined for all elements. A concentrated load P is dynamically applied at the joint B acting downwards, while the loading eccentricity is implemented in the form of a concentrated moment applied at the same joint of magnitude $M = -Pe$. In Fig. 4, the finite element model of a rectangular two-bar frame, created by Superdraw, is shown.

Next, with the aid of "Nonlinear Decoder" editor of Algor, where the solution technique and the loading parameters are set. Geometrical nonlinearity with large displacements is defined for the model, and the updated Lagrange method

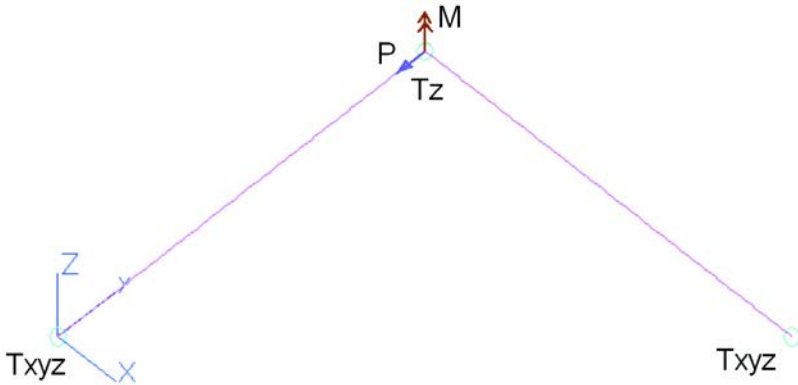

FIG. 4. Finite element model of a rectangular two-bar frame.

for solution of the nonlinear problem is chosen. Finally, the loading step size as well as the tolerance value is defined. Execution of the Nonlinear Decoder creates the input file for the nonlinear FE solver.

The nonlinear solver of the Algor package is used and the nonlinear solution is performed. The results are stored in the output file and can be viewed with the "Nonlinear Superview" editor of Algor. In Fig. 5, one can see the postbuckling deformation for the rectangular frame with eccentricity $e = 0.01$ obtained via the finite element method.

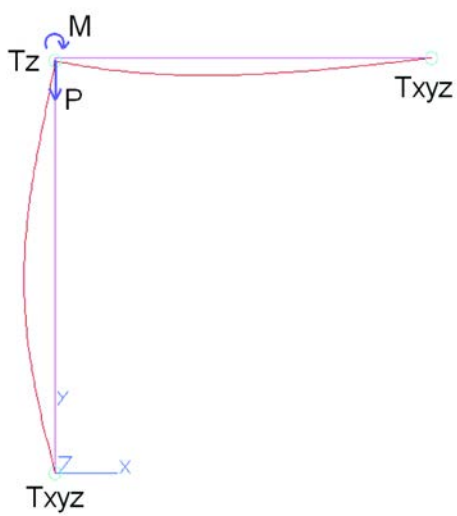

FIG. 5. Dynamic buckled shape of the rectangular frame with $e = 0.01$ obtained by FEM.

It is worth to notice that for the cases of frames with initial imperfections, there occurs inadequacy or unreliability of the results obtained via finite ele-

ment analyses, which can be safely established by using the proposed technique which is essentially analytic. More specifically, using the conservation of energy principle for conservative systems, we see that after a large number of cycles (time-steps) the total potential energy V and the kinetic energy K do not cancel each other, as could be expected from the theoretical analysis. This justifies the slight deviation observed between the results obtained by FEM and the ones obtained analytically.

6. Concluding remarks

The most important conclusions of this study dealing with the nonlinear dynamic buckling response of a rectangular imperfect two-bar non-sway frame with various loading eccentricities, can be summarized as follows:

1. A systematic, comprehensive and readily applicable method for establishing the dynamic buckling loads of imperfect (due to loading eccentricity frames) is thoroughly discussed. This is facilitated by considering the total potential energy (TPE) as a function of the two axial bar forces. Thus, the continuous system (frame) is reduced to a 2 degrees-of-freedom system.
2. A qualitative discussion for seeking the dynamic buckling load based on geometrical considerations involving the TPE surface is properly established.
3. A direct and easily employed evaluation of the static critical buckling (limit point) load is established leading to very reliable results. To this end, the numerical part is appreciably reduced. Moreover, the analytical part can also be reduced if symbolic manipulation is employed.
4. The dynamic buckling loads for non-sway two-bar frames corresponding to a certain (non-zero) loading eccentricity are obtained for various geometrical parameters. The results are compared with the numerical ones obtained by a nonlinear FEM analysis.
5. The proposed approach proved to be very reliable and the computational effort is drastically reduced in case of multi-parameter analyses.

References

1. W. T. Koiter, *On the Stability of Elastic Equilibrium*, PhD Thesis presented to the Polytechnic Institute of Delft, The Netherlands 1945 (English translation NASA TT-F-10833, 1967).

2. J. M. T. Thompson and G. W. Hunt, *A general Theory of Elastic Stability*, John Wiley & Sons, London 1973.

3. G. I. Ioannidis, I. G. Raftoyiannis and A. N. Kounadis, *Nonlinear Buckling of Imperfect Systems with Symmetric Imperfections*, Archive of Applied Mechanics, **73**, 711–717, 2004.

4. D. O. Brush and B. O. Almroth, *Buckling of Bars, Plates, and Shells*, McGraw-Hill, New York, NY 1975.

5. A. N. Kounadis, *Dynamic Buckling of Simple Two-Bar Frames Using Catastrophe Theory*, Int. J. Non-Linear Mech., **37**, 1249–1259, 2002.

6. A. N. Kounadis, G. I. Ioannidis and X. Lignos, *Stability Analysis of a Two-Bar Frame Using Catastrophe Theory*, Proc. Eurosteel '02, Coimbra, Portugal, **1**, 149–61, 2002.

7. G. A. Simitses, *Elastic Stability of Structures*, Prentice Hall Inc., Englewood Cliffs, New Jersey 1976.

8. A. N. Kounadis, J. Giri and G. A. Simitses, *Nonlinear Stability Analysis of an Eccentrically Loaded Two-Bar Frame*, J. Appl. Mech., ASME, **44**, 4, 701–706, 1977.

9. G. A. Simitses and A. N. Kounadis, *Buckling of Imperfect Rigid-Jointed Frames*, J. Eng. Mech. Div., ASCE, **104**, EM3, 569–586, 1978.

10. A. N. Kounadis, *An Efficient Simplified Approach for the Nonlinear Buckling Analysis of Frames*, AIAA J., **23**, 8, 1254–1259, 1985.

11. A. N. Kounadis, *Efficiency and Accuracy of Linearized Postbuckling Analyses of Frames based on Elastica*, Int. J. Solids and Structures, **24**, 11, 1097–1112, 1988.

12. S. P. Timoshenko and J. M. Gere, *Theory of Elastic Stability*, McGraw-Hill, New York, NY 1961.

13. S. Wolfram, *Mathematica*, 4th ed., Version 4, Cambridge University Press, UK 1999.

14. G. I. Ioannidis and I. G. Raftoyiannis, *A Simplified Nonlinear Stability Analysis of an Imperfect Rectangular Two-Bar Frame*, Computational Mechanics, **35**, 2, pp. 127–133, 2004.

15. C. C. Spyrakos and I. G. Raftoyiannis, *Linear and nonlinear finite element analysis in engineering practice*, Algor Publ. Div., Pittsburgh, PA 1997.

16. A. N. Kounadis, *A Geometric Approach for Establishing Dynamic Buckling Loads of Autonomous Potential 2-DOF Systems*, J. Appl. Mech., ASME, **66**, 1, 55–61, 1999.

17. I. G. Raftoyiannis, G. T. Constantakopoulos, G. T. Michaltsos and A. N. Kounadis, *Dynamic Buckling of a Simple Geometrically Imperfect Frame using Catastrophe Theory*, Int. J. Mechanical Sciences, **48**, 1021–1030, 2006.

Received March 17, 2008; revised version November 24, 2008.